Available online at www.sciencedirect.com
ScienceDirect
Journal of Catalysis 243 (2006) 57–63
JOURNAL OF CATALYSIS
www.elsevier.com/locate/jcat

Silylation of [Nb]-MCM-41 as an efficient tool to improve epoxidation activity and selectivity

J.M.R. Gallo, H.O. Pastore, U. Schuchardt *

Instituto de Química, Universidade Estadual de Campinas, P.O. Box 6154, 13084-971 Campinas SP, Brazil

Received 6 June 2006; revised 6 July 2006; accepted 6 July 2006

Available online 21 August 2006

Abstract

Well-ordered [Nb]-MCM-41 was synthesized at room temperature with essentially all niobium present in the sample substituted into the silica framework. The material was calcined and then silylated using hexamethyldisilazane (HMDS). Both calcined and silylated materials were characterized by X-ray diffraction (XRD), diffuse reflectance UV–vis, inductively coupled plasma emission (ICP-OES), infrared spectroscopy (FTIR), N_2 adsorption at low temperatures, thermogravimetry (TG), and nuclear magnetic resonance of ^{29}Si with magic-angle spinning (NMR-MAS). The materials were used as catalysts in the epoxidation of *cis*-cyclooctene with *tert*-butyl hydroperoxide (TBHP) and 70 wt% aqueous hydrogen peroxide as oxidants, to verify the influence of the silylation on the activity and selectivity. It was observed that the silylated material was more active for both oxidants, reaching 62% conversion and 94% selectivity after 48 h with TBHP and 13% conversion and 80% selectivity after 5 h with aqueous hydrogen peroxide.
© 2006 Elsevier Inc. All rights reserved.

Keywords: Nb-MCM-41; Silylation; Hexamethyldisilazane; Epoxidation; *Cis*-cyclooctene

1. Introduction

At the start of the 1990s, researchers from the Mobil Research and Development published the first results on a family of mesoporous molecular sieves called M41S. The members of this family present hexagonal (MCM-41), cubic (MCM-48), or lamellar (MCM-50) structures (Mobil Composition of Matter) [1,2]. MCM-41 is currently one of the most widely studied synthetic mesoporous materials, due to its structural simplicity and the ease of modifying its physical-chemistry properties. The more important characteristics of MCM-41 are well-defined pore shape and size, narrow pore size distribution, high ordering in the micrometric scale, adjustable pore size (1.5–20 nm), high pore volumes (>0.6 cm^3 g^{-1}), high adsorption capacity (64 wt% of benzene at 50 Torr and 25 °C), high surface area (700–1500 m^2 g^{-1}), large quantity of internal silanol groups (40–60%), reactive surface, possibility of aluminum-free synthesis, and high thermal, hydrothermal, chemical, and mechanical stability [3]. The main applications of MCM-41 are as a heterogeneous catalyst, as a support for catalysts, for heterogenezation of homogeneous catalysts, as a molecular host, and in adsorption processes [3].

Acid sites are generated by isomorphous substitution of silicon in tetrahedral positions by trivalent metals (e.g., boron, gallium, aluminum, and iron) [4–7]. With the incorporation of these cations, the framework of the [M^{3+}]-MCM-41 presents negative charges that can be compensated by cations such as sodium, calcium, potassium, proton (Brønsted acidity), and others. It also allows ion exchange, which can provide the material with new characteristics; an example is the cesium ion-exchanged [Al]-MCM-41, which presents Lewis basicity [8,9]. Furthermore, the incorporation of tetravalent metals, such as titanium, vanadium, zirconium, and lead, generates the neutral [M^{4+}]-MCM-41, which are redox catalysts and can be used in selective oxidation [10–13]. The high quantity of silanol groups in MCM-41 allows the anchoring of classical homogeneous catalysts [8,9,14–16]. Schuchardt and co-workers [17,18] immobilized propylamine complexes of iron and copper and guanidines into MCM-41 for the oxidation of cyclohexane and the aldolysis of benzaldehyde with acetone, respectively. Another impor-

* Corresponding author. Fax: +55 19 37883023.
E-mail address: ulf@iqm.unicamp.br (U. Schuchardt).

0021-9517/$ – see front matter © 2006 Elsevier Inc. All rights reserved.
doi:10.1016/j.jcat.2006.07.002

tant use of MCM-41 is in the encapsulation of metals, metal oxides, semiconductors, clusters, and nanowires. The synthesis of carbon nanowires and polyanilines into the MCM-41 channels was a revolution in the chemistry of materials [3].

The [Nb]-MCM-41 synthesis was published for the first time in 1997 by the groups of Ziolek [19,20] and Ying [21]. Ziolek and co-workers [19] compared [Al]- and [Nb]-MCM-41 acidity by FTIR; the analysis with adsorbed pyridine indicated that [Al]-MCM-41 had higher Brønsted acidity and lower Lewis acidity. There is a certain level of uncertainty about [Nb]-MCM-41 Lewis acidity, because the quantity of niobium oxide dispersed in the channels is unknown. In the same paper, H[Al]- and H[Nb]-MCM-41 were used in the decomposition of isopropanol and in the cracking of cumene. In both reactions, the H[Al]-MCM-41 was more active, confirming its higher Brønsted acidity. In a subsequent paper, Ziolek and Nowak [20] characterized the [Nb]-MCM-41, which showed low structural ordering. Zhang and Ying [21] synthesized [Nb]-MCM-41 with good structural ordering and proved by diffuse reflectance UV–vis spectroscopy that all niobium present in the solid was incorporated into the silica framework.

Ziolek and co-workers [22] also studied the oxidative properties of [Nb]-MCM-41 and concluded that the material is active in the oxidation of thioethers with H_2O_2 when the species Nb-O^- is present (formed by dehydration). The same group performed epoxidation of cyclohexane using [Nb]-MCM-41 containing 6 wt% of niobium and hydrogen peroxide 34% in acetonitrile, reaching 45% conversion after 11 h at 45 °C [23]. In an earlier article comparing [Nb]-e [Ti]-MCM-41 activity in the epoxidation of *cis*-cyclooctene, we showed that [Nb]-MCM-41 with 1.5 wt% of niobium and 69.4% *tert*-butyl hydroperoxide in cyclohexane led to *cis*-cyclooctene epoxide with 18.9% conversion after 10 h, whereas [Ti]-MCM-41 led to 24.9% conversion under the same conditions [24]. Vetrivel and Pandurangan [25] showed that the [Nb]-MCM-41 obtained by postsynthesis niobium incorporation is active in the oxidation of the *meta*-toluidine with molecular oxygen with 41.1% conversion, giving 55.5% of *meta*-amine benzoic acid and 41.6% of *meta*-amine benzaldehyde at 250 °C.

Corma and co-workers [26] showed that silylation of [Ti]-MCM-41 with hexamethydisilazane (HMDS) improved the catalyst activity in the epoxidation. Silylation involves the substitution of –OH groups of the MCM-41 surface by –$OSiR_3$. This makes the material more hydrophobic and thus improves its interaction with the substrate (alkene) while diminishing the affinity for the product (epoxide, alcohols, ketones). In this paper we report silylation of the [Nb]-MCM-41 as a tool for improving the activity of this material in the epoxidation of *cis*-cyclooctene.

2. Experimental

2.1. [Nb]-MCM-41 synthesis

[Nb]-MCM-41 synthesis was carried out by dissolving 0.50 g (1.37 mmol) of cetyltrimethylammonium bromide (CTMABr, Vetec) in a mixture of 2.5 ml (7 mmol) of tetramethylammonium hydroxide (TMAOH 25% in water, Aldrich) and 100.0 ml of distillated water. Tetraethyl orthosilicate (TEOS, Aldrich, 2.5 ml, 11 mmol) was added, and when the condensation of the TEOS began (after 1–2 min), 0.057 g (0.15 mmol) of ammonium niobium oxalate [NH_4[NbO-$(C_2O_4)_2(H_2O)_2$]3H_2O, CBMM] was added. The reaction mixture was stirred for 24 h at room temperature, and the solid thus obtained was filtered and washed with distilled water until the pH of the filtrate was neutral. The solid was dried overnight at air and then calcined at 500 °C (heating rate of 1 °C min^{-1}) for 1 h under nitrogen flow and overnight under air flow (both at 100 ml min^{-1}). The molar composition was SiO_2: $0.075Nb_2O_5$:$0.06(CTMA)_2O$:$4.875(TMA)_2O$:$485.76H_2O$.

2.2. [Nb]-MCM-41 silylation

Previously calcined [Nb]-MCM-41 (1 g) was heated to 250 °C under vacuum for 12 h. It was then dispersed in 15.0 ml of a 5 wt% solution of hexamethyldisilazane (HMDS, Aldrich) in dry toluene, under inert atmosphere. The dispersion was stirred for 7 h at 120 °C. The solid was filtered and washed with 100 ml of dry toluene and 200 ml of anhydrous ethanol.

2.3. Characterization

The X-ray diffractograms were recorded with a Shimadzu XRD-6000 diffractrometer, using Cu$K\alpha$ radiation at 40 kV and 30 mA and a graphite monochromator. The diffuse reflectance on UV–vis spectra were recorded at a UV/vis/NIR Perkin–Elmer Lambda-9 series 1645 spectrometer using $BaSO_4$ as a blank. The elemental analysis of carbon, hydrogen, and nitrogen was performed with a CHN S/O Analyser 2400, series II (Perkin–Elmer). The infrared spectra were obtained in a Bomen MB-Series spectrometer using KBr pellets and a resolution of 4 cm^{-1}. Thermogravimetry was performed in a thermogravimetric balance (TA 5100, TA Instruments, module TG 2050) at a heating rate of 10 °C min^{-1} under argon or air flow. The quantification of niobium in the [Nb]-MCM-41 was done by inductively coupled plasma (ICP) emission using a Spectroflame Modula (Spectro Co., Germany), at a wavelength of 309.418 nm. Nuclear magnetic resonance of ^{29}Si with magic-angle spinning spectra was performed in a Bruker AC 300/P. The samples were spun at 4.5 kHz in a zirconia rotor with 10-s intervals between the pulses and using tetramethylsilane as reference. The spectra were obtained after proton decoupling. The adsorption/desorption of nitrogen was carried out at −196 °C in a Micromeritics ASAP 2010. The samples were previously treated under high vacuum at 150 °C for 12 h.

2.4. Solvent-free epoxidation of cis-cyclooctene using tert-butyl hydroperoxide

To a two-necked, 10-ml, round-bottomed flask, 1.160 g (10 mmol) of *cis*-cyclooctene (Aldrich), 0.325 g (2.5 mmol) of dibutyl ether (internal standart, Aldrich), 1.95 g (15 mmol) of *tert*-butyl hydroperoxide, 69.4% in cyclohexane (TBHP, Nitrocarbono S.A.), and 100 mg of [Nb]-MCM-41 (1.20 ×

10^{-2} mmol of niobium analyzed by ICP-OES) were added. The reaction mixture was stirred for 48 h at 80 °C. The reactions were monitored by analyzing aliquots obtained at different reaction times, using an Hewlett–Packard HP 5890 Series II gas chromatograph equipped with an HP Ultra 2 capillary column (50 m × 0.2 mm × 0.33 μm film thickness; cross-linked 5% phenyl methyl silicone) and a flame ionization detector (FID). Unknown products were identified using an HP 5970 Series mass selective detector (MSD) coupled to the same gas chromatograph.

2.5. Epoxidation of cis-cyclooctene using 70 wt% aqueous hydrogen peroxide

The reaction was carried out as described in Section 2.3, with the following modifications: A two-necked, 50-ml, round-bottomed flask was used; 1.46 g (30 mmol) of 70 wt% aqueous hydrogen peroxide (Peroxidos do Brasil) was used instead of TBHP; and 10 ml of ethyl acetate (Merck) was used as the solvent. The reaction mixture was stirred for 24 h at 80 °C.

3. Results and discussion

3.1. XRD

Fig. 1 shows the XRD of as-made, calcined, and silylated [Nb]-MCM-41. A typical X-ray diffractogram of a MCM-41 shows 4 peaks at low angles [27]. The first, and most intense, of these peaks, is at approximately at $2\theta = 2°$ (100); the other reflections, at (110), (200), and (210), appear in the range of $3° < 2\theta < 10°$. These four peaks can be indexed to a hexagonal unit cell ($a = 2d_{100}/(3)^{1/2}$) [27]. The values of 2θ for each of the Miller planes and the calculated values of d_{hkl} and a_0 are given in Table 1.

The data in Table 1 show that a_0 was smaller for the calcined sample than for the as-synthesized sample, indicating that the thermal process causes shrinkage of the framework. This situation remained the same after silylation. In the X-ray diffractogram of the silylated sample, the peaks corresponding to the (110) and (200) diffractions decreased in intensity, suggesting that the partial loss of the hexagonal symmetry of the sample [3].

3.2. Diffuse reflectance UV–vis spectroscopy

According to Prakash and Kevan [28], the diffuse reflectance UV–vis spectrum of isolated niobium ions in the silica framework of molecular sieves (0.1%) presents a band at 220 nm. Tanaka et al. [29] attributed this band to Nb_2O_5 (0.1%) dispersed in molecular sieves. This lack of agreement in the literature shows that the electronic spectrum of niobium incorporated into silica remains controversial. In a recent report [24,30], we attributed the band at 235 nm to niobium substituted in the MCM-41 silica framework in isolated sites and the band at 290 nm to the formation of Nb_2O_5 dispersed in the channels. We also proved that only the isolated niobium, which absorbs at 235 nm, is active in the epoxidation of *cis*-cyclooctene, and, as already known, the niobium oxide is not active [31]. Fig. 2 shows the diffuse reflectance UV–vis spectra of the as-made, calcined, and silylated samples. A strong band at 235 nm is present, along with a minor contribution at 290 nm, from aggregated sites. This result is very important from the standpoint of catalytic oxidation, because materials with dispersed oxides

Table 1
Values of the observed 2θ and calculated values of d_{hkl} and a_0

Sample	hkl	2θ (°)	d_{hkl} (nm)[a]	a_0 (nm)[b]
As-made	100	2.36	3.74	4.89
	110	4.07	2.17	
	200	4.69	1.88	
	210	6.18	1.43	
Calcined	100	2.60	3.40	4.57
	110	4.45	1.98	
	200	5.15	1.72	
	210	–	–	
Silylated	100	2.60	3.40	4.57
	110	4.40	2.01	
	200	5.12	1.69	
	210	–	–	

[a] $\lambda = 2d \sin\theta$.
[b] a_0 is the linear coefficient of the graph d versus $[3/4(h^2 + k^2 + hk)]^{1/2}$.

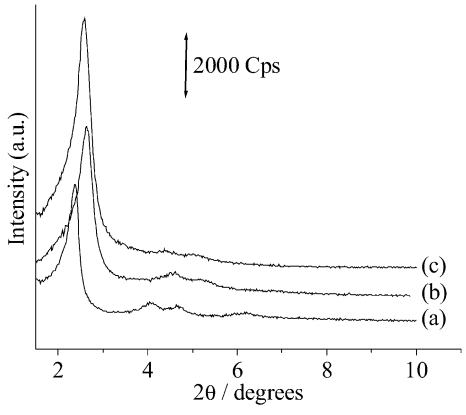

Fig. 1. X-ray diffractograms of (a) as-made, (b) calcined, and (c) silylated [Nb]-MCM-41.

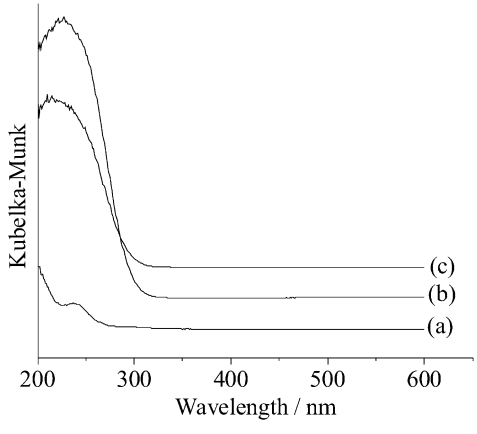

Fig. 2. Diffuse reflectance UV–vis spectra of the (a) as-made, (b) calcined, and (c) silylated sample.

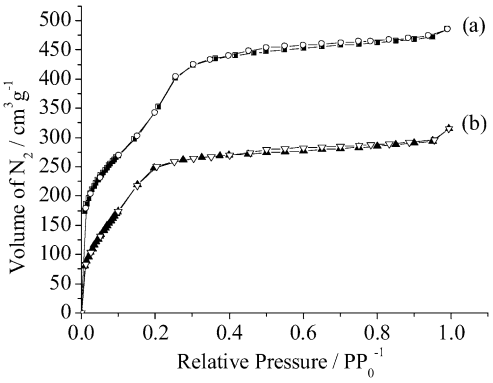

Fig. 3. N_2 isotherms of (a) calcined and (b) silylated [Nb]-MCM-41. Full symbols: adsorption; open symbols: desorption.

Table 2
Pore characteristics of the calcined and silylated [Nb]-MCM-41

Sample	V_P ($cm^3\ g^{-1}$)	S_{BET} ($m^2\ g^{-1}$)	D_P (nm)	W (nm)
Calcined	0.75	1157	2.60	2.26
Silylated	0.48	923	2.11	2.46

tend to be less selective, catalyzing both the isomerization and epoxide ring-opening reaction.

3.3. Nitrogen adsorption at low temperatures

The N_2 adsorption/desorption isotherms of the calcined and silylated samples are shown in Fig. 3. Using the Brunauer–Emmett–Teller (BET) equation, the values of pore volume and diameter were calculated. The values of wall thickness were calculated from the value of pore diameter and the unit cell parameter, a_0 (see Table 1). These values are given in Table 2.

Three stages of adsorption and desorption of nitrogen can be seen in the isotherm of the calcined sample: (1) adsorption at low relative pressure, corresponding to the adsorption of monolayers of nitrogen on the pore walls; (2) a light inflection point at intermediate relative pressure due to capillar condensation in the pores; and (3) a plateau at higher relative pressures, associated with the adsorption of multilayers on the material surface [32]. In the silylated sample, the second stage is very subtle. These types of isotherms are usually classified as a mixture of type IV and type I. According to Biz e Occelli [32], the decrease in $PP_0{}^{-1}$ where the inflection point is found is directly proportional to pore narrowing. In the silylated sample, the reduction was already expected because hydroxyl groups were substituted by bulkier trimethylsilyl groups. This is the reason for diminished pore volumes, pore diameters, and surface area in silylated samples compared with the calcined sample. The inflection at relative pressures above 0.9 is due to the formation of pores in the interstices of the particles [33].

3.4. IR spectroscopy

The FTIR spectra of the samples are shown in Fig. 4. The FTIR spectra of [Nb]-MCM-41 present wide bands at approximately 3400 and 1630 cm^{-1}, assigned to the stretching and

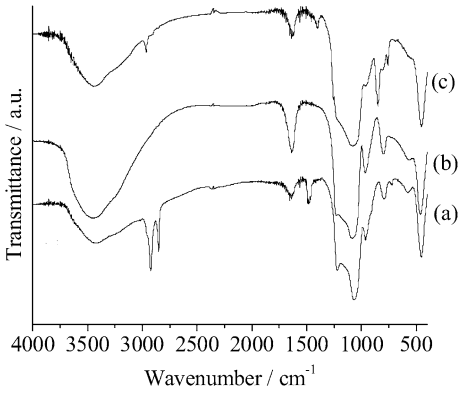

Fig. 4. FTIR spectra of the (a) as-made, (b) calcined, and (c) silylated [Nb]-MCM-41.

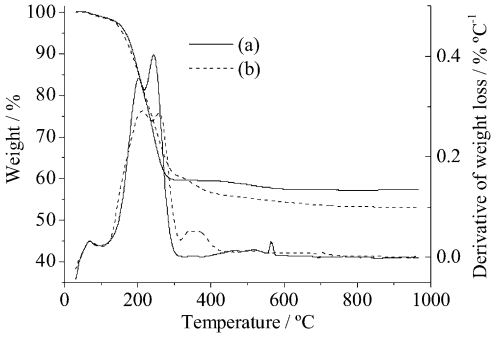

Fig. 5. TG and DTG of the (a) as-made MCM-41 and (b) [Nb]-MCM-41.

bending modes of the O–H group, respectively (Fig. 4) [34]. In the spectrum of the as-made sample (Fig. 4a), bands at 2921 and 2852 cm^{-1} are due to the C–H stretching of the CH_3 and CH_2 groups of the $CTMA^+$ groups, along with the band at 1488 cm^{-1} due to the bending of H–C–H [34]. In the region between 1400 and 450 cm^{-1}, the bands are assigned to the fundamental vibrations of the MCM-41 framework: the asymmetric and symmetric stretching of the Si–O–Si bond at 1050 and 800 cm^{-1} and the Si–O stretching of the Si–OH groups at 950 cm^{-1} [35]. The band at 457 cm^{-1} is characteristic of silica compounds and corresponds to the bending of the O–Si–O groups [36]. A very weak band at 574 cm^{-1} is due to the presence of the ordered silica structure [36]. This band decreased in the calcinated and silylated samples, confirming the results of the X-ray diffractograms. These bands due to organic moieties reappeared in the spectrum of the silylated sample, confirming the success of the procedure [37].

3.5. TG and DTG

To understand the best temperature sequence for calcination, we examined the thermogravimetric curve. Fig. 5 shows the TG and DTG results for the as-made MCM-41 [38] (curves a) and as-made [Nb]-MCM-41 (curves b). The first mass loss at temperatures below 120 °C is due to water release (2.3% for both). Between 100 and 318 °C, a weight loss of 39.7% for [Nb]-MCM-41 and a 40.6% for MCM-41 can be seen; this can be assigned to the Hoffmann degradation of CTMABr [39]. Between 318 and 422 °C, a 1.2% mass loss is seen only for the

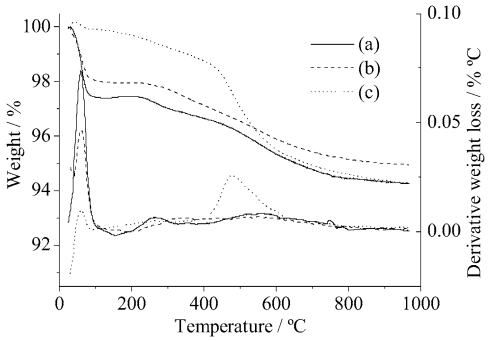

Fig. 6. TG and DTG of the (a) calcined MCM-41, (b) calcined [Nb]-MCM-41, and (c) silylated [Nb]-MCM-41.

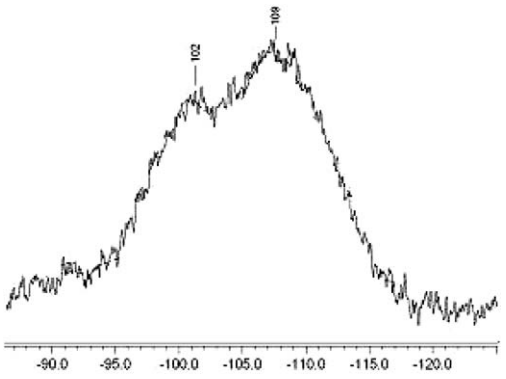

Fig. 7. NMR-MAS spectrum of the calcined [Nb]-MCM-41.

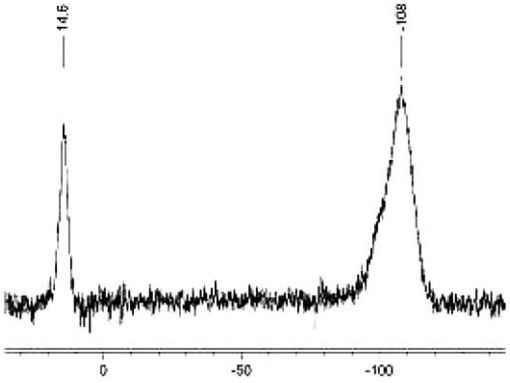

Fig. 8. NMR-MAS spectrum of the silylated [Nb]-MCM-41.

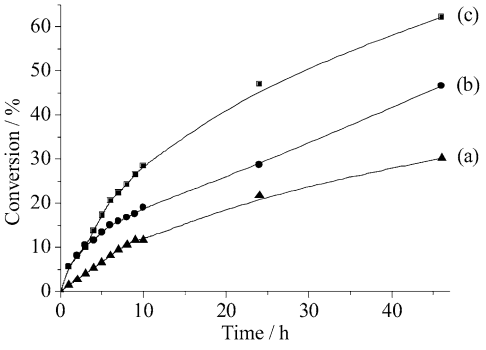

Fig. 9. Conversion as function of time for the epoxidation of *cis*-cyclooctene with *tert*-butyl hydroperoxide, (a) blank experiment, (b) calcined, and (c) silylated [Nb]-MCM-41.

as-made [Nb]-MCM-41. The same behavior has been reported for [Al]-MCM-41 by Beck et al. [1]. The effect that these authors described can also be used in the present material; the temperature of desorption and degradation of the organics in the higher temperature range is related to the association of the $CTMA^+$ with siloxy groups and Brønsted sites, the latter from the niobium substitution in the framework. The siloxy groups are stronger acids and should promote Hoffman degradation at lower temperatures [1].

For the as-made [Nb]-MCM-41, the mass loss was 44.77% up to 500 °C, representing 87.1% of the total amount of organics (total amount calculated by the TG under air). Thus, a large and substantial amount of organics was decomposed under N_2. Consequently, to eliminate as much CTMABr as possible without producing much water, all calcinations was performed by heating under nitrogen until 500 °C; only then, when most organics were either eliminated or had become carbon residue, was oxygen admitted to the system to burn carbon residues.

TG and DTG of the calcined MCM-41 (rehydrated at ambient atmosphere for a couple of hours) (Fig. 6a) show a loss of 2.6% due to desorption of water molecules up to 110 °C, 0.6% more than the [Nb]-MCM-41 (Fig. 6b). This result was expected, because in [Nb]-MCM-41, the niobyl species are bound to 2 or 3 silyl groups [24], thus reducing the amount of surface hydroxyls. As for the silylated sample (Fig. 6c), the water loss was reduced to 0.1%, proving that the silylation was efficient in hydrophobizing the [Nb]-MCM-41. At higher temperatures (>150 °C), degradation of the $Si(CH_3)_3$ groups occurred.

3.6. ^{29}Si NMR-MAS

The MAS-NMR spectrum of the calcined [Nb]-MCM-41 sample (Fig. 7) shows two large and partially overlapped signals corresponding to the Q^4 and Q^3 groups, at −109 and −102 ppm. The Q^3/Q^4 ratio is 0.55, slightly larger than the values reported in the literature for such materials as MCM-41 (0.44), [Ti]-MCM-41 (0.37), [V]-MCM-41 (0.35), and [Zr]-MCM-41 (0.38) [40].

In the MAS-NMR spectrum of the silylated sample (Fig. 8), the peak assigned to silicon Q^3 was largely diminished, because in the silylation it has been converted to silicon Q^4 [41,42]. The value of Q^3/Q^4 was as low as 0.05. A new peak at 14 ppm appeared after silylation, due to the Si nuclei in $Si(CH_3)_3$ groups, confirming that the silylation was successful [41,42].

3.7. Epoxidation of cis-cyclooctene

Results from the epoxidation of *cis*-cyclooctene using *tert*-butyl hydroperoxide (TBHP) as oxidant and calcined or silylated [Nb]-MCM-41 as catalyst are shown in Fig. 9. The silylated material was more active than the calcined [Nb]-MCM-41; this can be explained by the good interaction of the polar epoxide with the polar surface of the calcined [Nb]-MCM-41 compared with its poor interaction with the apolar reaction medium. Thus the epoxide remains in the [Nb]-MCM-41 chan-

nels, blocking the active catalytic sites. In the silylated [Nb]-MCM-41, the epoxide is more easily removed from the channels, thus increasing the activity of this material.

The selectivity for epoxide was 85% for the blank experiment (no-catalyst), 77% for the calcined [Nb]-MCM-41, and 94% for the silylated [Nb]-MCM-41, with corresponding initial turnover frequencies 11, 20, and 26 h^{-1}. These data reinforce the earlier-stated assumption that the epoxide remains inside the channels of calcined [Nb]-MCM-41, facilitating further transformation and diminishing selectivity. In the first 3 h, the reaction remained essentially the same whether using the calcined or silylated sample as the catalyst. After this, the calcined [Nb]-MCM-41 had a significant decrease in activity, caused by blockage of the catalytic sites by the byproducts. This effect was not observed in the silylated catalyst, the selectivity of which remained high.

The results for the epoxidation of *cis*-cyclooctene using 70 wt% aqueous hydrogen peroxide and ethyl acetate as solvent are shown in Fig. 10. The silylated [Nb]-MCM-41 was more active than the calcined [Nb]-MCM-41 in the first 10 h when 70 wt% aqueous hydrogen peroxide was used as oxidant, reaching 70 and 80% selectivity for the epoxide, respectively. The initial turnover frequencies were 15 h^{-1} for the calcined [Nb]-MCM-41 and 50 h^{-1} for the silylated [Nb]-MCM-41. In this reaction, hydrogen peroxide is consumed very rapidly; after 10 h for the calcined sample and 5 h for the silylated sample, almost all hydrogen peroxide was consumed, as determined by iodometric titration. The silylated sample degrades hydrogen peroxide more rapidly, probably due to the presence of ammonium ion or amine residues, which are byproducts of the silylation and consume hydrogen peroxide. An interesting observation is that in the first 3 h, the reaction using silylated [Nb]-MCM-41 was faster when using aqueous hydrogen peroxide than when using TBHP. The opposite occurred with the calcined [Nb]-MCM-41.

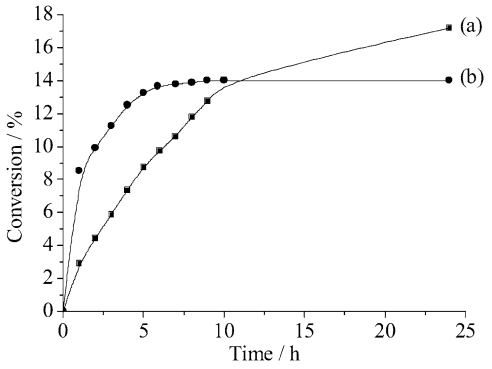

Fig. 10. Conversion as a function of time for the epoxidation of *cis*-cyclooctene with 70 wt% aqueous hydrogen peroxide, (a) calcined and (b) silylated [Nb]-MCM-41.

Comparing the catalysts described in this paper with other recently reported [24,43–46] (Table 2) verifies that for reactions using TBHP as oxidant, the silylated [Nb]-MCM-41 showed conversions comparable with those obtained with titanium, aluminum, manganese, and zirconium catalysts. However, in the reactions using aqueous hydrogen peroxide, [Nb]-MCM-41 rapidly decomposed the oxidant, leading to low final conversions compared with those of other catalysts (Table 3).

4. Conclusion

We report a new synthesis method for the preparation of [Nb]-MCM-41 at room temperature that leads to well-ordered material with the niobium inside the silica framework. This material was silylated with hexamethyldisilazane, maintaining a good structural ordering and keeping the niobium ions inside the silica framework. Both the silylated and calcined catalysts were characterized and used in the epoxidation of *cis*-cyclooctene with *tert*-butyl hydroperoxide 69.6% in cyclohexane or 70 wt% aqueous hydrogen peroxide as oxidant. The silylated sample was more active than the calcined sample in the epoxidation of *cis*-cyclooctene; however, the silylated sample decomposed faster with hydrogen peroxide, producing lower conversions than those obtained using *tert*-butyl hydroperoxide as oxidant.

Acknowledgments

The authors thank CNPq and CAPES for financial support. J.M.R.G. thanks FAPESP for a fellowship (process 03/09794-8) and Roberto Bineli Muterle and Fabio Fabri for helpful discussions.

Table 3
Activity of catalysts recently for the epoxidation of *cis*-cyclooctene. Results after 24 h of reaction

Catalyst	Oxidant	T (°C)	C[a] (%)	S[b] (%)	Initial TOF (h^{-1})
Ti-SBA-15 (8×10^{-5} mol of Ti) [43]	TBHP (70%)	70	98	100	–
	H_2O_2 (30% aq.)	70	50	100	–
Ti-SiO_2 (0.2 g) [44]	H_2O_2 (30% aq.)	80	36	100	4.2
[Ti]-MCM-41 [24]	TBHP (69.4%)	80	79	100	101
OMS-2 (50 mg) [45]	TBHP (70%)	60	59	100	1.97
Al_2O_3 (50 mg) [46]	TBHP (88%)	80	43	100	–
Al_2O_3–ZrO_2 (50 mg) [46]	TBHP (88%)	80	37	100	–
Al_2O_3–TiO_2 (50 mg) [46]	TBHP (88%)	80	54	100	–
ZrO_2–TiO_2 (50 mg) [46]	TBHP (88%)	80	41	100	–
Silylated	TBHP	80	62	94	26
[Nb]-MCM-41	H_2O_2	80	14	70	50

[a] Conversion: percentage of *cis*-cyclooctene converted into products.
[b] Selectivity: percentage of *cis*-cyclooctene oxide formed with respect to all products.

References

[1] J.S. Beck, J.C. Vartuli, W.J. Roth, M.E. Leonowicz, C.T. Kresge, K.D. Schmitt, C.T.W. Chu, D.H. Olson, E.W. Sheppard, S.B. McCullen, J.B. Higgins, J.L. Schlenker, J. Am. Chem. Soc. 114 (1992) 10,834.

[2] C.T. Kresge, M.E. Leonowicz, W.J. Roth, J.C. Vartuli, J.S. Beck, Nature 359 (1992) 710.

[3] P. Selvam, S.K. Bhatia, C.G. Sonwane, Ind. Eng. Chem. Res. 40 (2001) 3237.

[4] G.J. Kim, J.H. Shin, Catal. Lett. 63 (1999) 205.

[5] S.K. Badamali, A. Sakthivel, P. Selvam, Catal. Lett. 65 (2000) 153.

[6] A. Sakthivel, S.K. Badamali, P. Selvam, Micropor. Mesopor. Mater. 39 (2000) 457.

[7] A. Corma, V. Fornes, M.T. Navarro, J. Perez-Pariente, J. Catal. 148 (1994) 569.

[8] K.R. Kloetstra, M. van Laren, H. van Bekkum, J. Chem. Soc. Faraday Trans. 93 (1997) 1211.

[9] Y.V.S. Rao, D.E. De Vos, P.A. Jacobs, Angew. Chem. Int. Ed. 36 (1997) 2661.

[10] A. Corma, M.T. Navarro, J. Perez-Pariente, J. Chem. Soc. Chem. Commun. (1994) 147.

[11] W.A. Carvalho, P.B. Varaldo, M. Wallau, U. Schuchardt, Zeolite 18 (1997) 408.

[12] P.T. Tanev, M. Chibwe, T.J. Pinnavaia, Nature 368 (1994) 321.

[13] R.J. Mahalingam, S.K. Badamali, P. Selvam, Chem. Lett. (1999) 1141.

[14] J.V. Walker, M. Morey, H. Carlsson, A. Davidson, G.D. Stucky, A. Butler, J. Am. Chem. Soc. 119 (1997) 6921.

[15] X.G. Zhou, X.Q. Yu, J.S. Huang, L.S. Li, C.M. Che, Chem. Commun. (1999) 1789.

[16] S.G. Shyu, S.W. Cheng, D.L. Tzou, Chem. Commun. (1999) 2337.

[17] W.A. Carvalho, M. Wallau, U. Schuchardt, J. Mol. Catal. A Gen. 144 (1999) 91.

[18] R. Sercheli, R.M. Vargas, R.A. Sheldon, U. Schuchardt, J. Mol. Catal. A Gen. 148 (1999) 173.

[19] M. Ziolek, I. Nowak, J.C. Lavalley, Catal. Lett. 45 (1997) 259.

[20] M. Ziolek, I. Nowak, Zeolite 18 (1997) 356.

[21] L. Zhang, J.Y. Ying, AIChE J. 43 (1997) 2793.

[22] M. Ziolek, I. Sobczak, A. Lewandowska, I. Nowak, P. Decyk, M. Renn, B. Jankowska, Catal. Today 70 (2001) 169.

[23] I. Nowak, B. Kilos, M. Ziolek, A. Lewandowska, Catal. Today 78 (2003) 487.

[24] J.M.R. Gallo, I.S. Paulino, U. Schuchardt, Appl. Catal. A Gen. 266 (2004) 223.

[25] S. Vetrivel, A. Pandurangan, Catal. Lett. 99 (2005) 2005.

[26] A. Corma, M. Domine, J.A. Gaona, J.L. Jorda, M.T. Navarro, F. Rey, J. Perez-Pariente, J. Tsuji, B. McCulloch, L.T. Nemeth, Chem. Commun. (1998) 2211.

[27] P. Selvam, S.K. Bhatia, C.G. Sonwane, Ind. Eng. Chem. Res. 40 (2001) 3237.

[28] A.M. Prakash, L. Kevan, J. Am. Chem. Soc. 120 (1998) 13,148.

[29] T. Tanaka, H. Nojima, H. Yoshida, H. Nakagawa, T. Funabiki, S. Yoshida, Catal. Today 16 (1993) 297.

[30] J.M.R. Gallo, I.S. Paulino, U. Schuchardt, Stud. Surf. Sci. Catal. 154 (2004) 2945.

[31] I. Nowak, M. Ziolek, Chem. Rev. 99 (1999) 3603.

[32] S. Biz, M.L. Occelli, Catal. Rev. Sci. Eng. 40 (1998) 329.

[33] F. Rouquerol, J. Rouquerol, K. Sing, Adsorption by Powders and Porous Solids: Principles, Methodology and Applications, Academic Press, London, 1999.

[34] M.D. Alba, Z. Luan, J. Klinowski, J. Phys. Chem. 100 (1996) 2178.

[35] G. Centi, S. Perathoner, F. Trifirò, A. Aboukais, C.F. Aissi, M. Guelton, J. Phys. Chem. 96 (1992) 2617.

[36] B.C. Trasferetti, C.U. Davanzo, M.A. Bica de Moraes, Macromolecules 37 (2004) 459.

[37] S. Eufinger, W.J. van Ooij, K.D. Conners, Surf. Inter. Anal. 24 (1996) 841.

[38] I.S. Paulino, U. Schuchardt, Stud. Surf. Sci. Catal. 141 (2002) 43.

[39] A. Fonseca, J.B. Nagy, J.E.A. Asswad, R. Mostowicz, F. Crea, F. Testa, Zeolite 15 (1995) 259.

[40] E. Meretei, J. Halász, D. Méhn, Z. Kónya, T.I. Korányi, J.B. Nagy, I. Kiricsi, J. Mol. Struct. 651 (2003) 323.

[41] K.A. Koyano, T. Tatsumi, Y. Tanaka, S. Nakata, J. Phys. Chem. B 101 (1997) 9436.

[42] M.L. Pena, V. Dellarocca, F. Rey, A. Corma, S. Coluccia, L. Marchese, Micropor. Mesopor. Mater. 44 (2001) 345.

[43] F. Chiker, F. Launay, J.P. Nogier, J.L. Bonardet, Green Chem. 5 (2003) 318.

[44] J.M. Fraile, J.I. Garcıa, J.A. Mayoral, E. Vispe, J. Catal. 189 (2000) 40.

[45] R. Ghosh, Y.C. Son, V.D. Makwana, S.L. Suib, J. Catal. 224 (2004) 288.

[46] R.F. Farias, U. Arnold, L. Martınez, U. Schuchardt, M.J.D.M. Jannini, C. Airoldi, J. Phys. Chem. Solids 64 (2003) 2385.